Journal of Non-Crystalline Solids 440 (2016) 70–75

Contents lists available at ScienceDirect

Journal of Non-Crystalline Solids

journal homepage: www.elsevier.com/locate/jnoncrysol

Adsorption of CsCl on porous SiO_2 glass surface: experimental results and ab-initio calculations

D.C. Lago [a], M. Nuñez [b,c,*], M.O. Prado [a,b,d]

[a] Departamento Materiales Nucleares, Centro Atómico Bariloche, Comisión Nacional de Energía Atómica, Argentina
[b] Consejo Nacional de Investigaciones Científicas y Técnicas, Argentina
[c] Instituto de Ciencias Basicas-Universidad Nacional de Cuyo, Argentina
[d] Instituto Balseiro (Universidad Nacional de Cuyo - Comisión Nacional de Energía Atómica), Argentina

ARTICLE INFO

Article history:
Received 9 September 2015
Received in revised form 8 February 2016
Accepted 23 February 2016
Available online xxxx

Keywords:
Porous silica
Adsorption
Glass
Density functional

ABSTRACT

The disposal of nuclear wastes is an issue of global concern due to the physicochemical and radiologic properties of some isotopes. Cesium radionuclides exhibit high solubility and some of them pose a long half-life. This work focuses on the study of Cs^+ adsorption on the surface of a porous silica glass. Adsorption experiments were done at room temperature using aqueous solutions with concentrations of 0.1 and 0.5 M of CsCl at pH = 5 and surface area to volume of 0.1 cm^{-1}. In these conditions, 14 and 18 $mgCs/gSiO_2$ were adsorbed, respectively. The adsorbed quantity of Cs^+ was determined by atomic absorption spectroscopy (AAS) analyzing the quantity of Cs^+ contained in the solution before and after adsorption experiments. The Cs^+/Cl^- ratio at a glass cross section surface, determined by energy dispersive spectroscopy analysis, is near 6. In addition, first principle calculations were performed, in order to determine charge transfer and location of the active sites for Cs^+ and Cl^-. Adhesion energy values are presented, which explain the experimental values found for the Cs^+/Cl^- concentration ratio at the silica glass surface. The parameters calculated from experimental and ab-initio calculations results were used to explain the adsorption mechanism.

1. Introduction

The need for materials, processes and methods for immobilizing radioactive isotopes in powder samples with long term stability and corrosion resistance has led to the use of ceramic matrices. Indeed, a large body of studies has been done on glasses and ceramics as matrices for containing radioisotopes [1–3]. Among the constituents of nuclear wastes, cesium stands out for its large water solubility and high vapor pressure at moderated high temperatures. In particular, Cesium 134, Cesium 135 and Cesium 137 exhibit high solubility and half-life of 2.06, $23 \cdot 10^6$ and 30.17 years, respectively. Furthermore, because of its chemical similarity to potassium, cesium is readily assimilated by terrestrial and aquatic organisms [4].

Controlled-pore silica glasses have found wide application for adsorption of ions, molecules, proteins and nucleic acids [5]. Because of its large surface area, controllable pore diameter, and chemical corrosion resistance, the porous silica glass is a promising material for nuclear wastes immobilization. Moreover, after ion adsorption, it allows sintering at temperatures about 1000 °C, in order to drastically decrease its exposed area [1,6]. Therefore it is of particular interest, to understand the behavior of this material, potentially capable of removing heavy and radioactive metals from industrial effluents and immobilizing them after sintering.

From the chemical point of view, main possible reactions for Cs^+ and Cl^- ions adsorption on the silica surface are showed by Eqs. (1) and (2):

$$\equiv Si - OH + M^{z+} \leftrightarrow \equiv Si - OM^{(z-1)+} + H^+ \quad (1)$$

$$\equiv Si - OH + A^{n-} \leftrightarrow \equiv Si - A^{(n-1)-} + OH^- \quad (2)$$

where M^{z+} is an atom or group of atoms that lost z electrons and A^{n-} is an atom or group of atoms that gained z electrons.

From the physical point of view, there are different sites where Cs^+ ions can be bonded, each one with different adsorption energy value. The same can be said for Cl^- attachment sites.

First principle calculations based on Density Functional Theory (DFT) have been widely used in modeling surface structures reactivity. Recently, these methods have been successfully used to investigate the interaction of carboxyl containing molecules with silica surface [7–9]. A slab model of the SiO_2 surface was built in order to understand the experimental results. Different guess sites for atom attachment were selected and the different adsorption energies for the involved atoms sites were calculated using DFT. We focused on energetics of

* Corresponding author at: Consejo Nacional de Investigaciones Científicas y Técnicas, Argentina.

http://dx.doi.org/10.1016/j.jnoncrysol.2016.02.020
0022-3093/

the interaction between the surface and CsCl and calculated the energy cost of removing each of the atoms from the clean hydroxylated surface.

2. Experimental methods

2.1. Sodium borosilicate glass preparation

A sodium borosilicate glass was prepared with composition: 65.6 wt.% SiO_2, 6.0 wt.% Na_2O, 27.8 wt.% B_2O_3 and 0.6 wt.% Al_2O_3. First, a mixture of high purity oxide precursors was homogenized in a rotating mill and melted in a platinum crucible for 2 h at 1600 °C. Afterwards, the melt was poured on a stainless steel plate and immediately splat-cooled with a second steel plate obtaining homogeneous transparent glass slabs with no visible symptoms of glass–glass separation.

2.2. Porous silica sintered matrix preparation

A fraction of the glass slabs was milled and sieved to obtain a powder with a particle size between 25 and 35 μm. Cylindrical powder compacts were produced by uniaxial pressing the powder at 0.5 MPa for 30 s. The dimensions of the obtained cylinders were approximately 2 mm in height and 1 mm in diameter. Finally, the compacts were partially sintered at 700 °C for 2 h, simultaneously developing a liquid–liquid phase separation.

The selected composition for the glass locates the sample inside a miscibility gap of the phase diagram. Consequently, during the sintering heat treatment, the sample is separated in glassy phases, one of almost pure SiO_2 and the other mainly composed of Na_2O-B_2O_3 [10]. The sintered compacts were leached in deionized water at 90 °C during 72 h and afterwards another 72 h in hydrochloric acid 1 M at room temperature. The Na_2O-B_2O_3 rich phase was eliminated from the sample during leaching. Nanometric porosity was generated by phase separation and leaching and micrometric porosity by partial sintering of the powder as in [1]. The pore size distribution of the samples shows that they have tri-modal pore distribution: large pores between 100 and 300 nm, medium sized pores at around 20 nm and small pores with diameters of less than 10 nm, as measured by Hg porosimetry and N_2 adsorption [1].

The remaining porous SiO_2 matrices were characterized chemical and morphologically using scanning electron microscopy (SEM).

2.3. Adsorption experiments

A stock solution of CsCl in water, with a concentration 1 M, was prepared by dissolving analytical grade metal chloride in deionized water. Then, it was diluted to obtain standard solutions of CsCl 0.1 and 0.5 M. Each of six pre-weighed porous matrix cylinders was placed in an individual vial with about 1 ml of a 0.1 M cesium chloride aqueous solutions at pH = 5, solid to solution ratio of 0.05 $g \cdot L^{-1}$, surface area to volume ratio 0.1 cm^{-1} and without mechanical agitation. After 7, 24 and 48 h, the porous matrices were removed from a pair of them (duplicated measurements) and the cesium concentration in the aqueous solution measured by atomic absorption spectroscopy (AAS). The same procedure was used with the 0.5 M solution. Cesium content and distribution concentration at the glass surface and in a cross section of the glass matrix were determined by energy-dispersive spectroscopy (EDS).

2.4. Computational details

The details of the adsorption mechanisms were investigated by electronic structure calculations within the framework of the Density Functional Theory (DFT) [11]. We used mainly the Quantum ESPRESSO code (QE) [12] that uses a plane wave basis to describe the electronic wave functions and ultrasoft pseudopotentials to represent the interaction between electrons and ions [13]. The exchange and correlation potential was considered at the level of the Generalized Gradient Approximation (GGA) based on the Perdew–Burke–Ernzerhof (PBE) expression [14–15]. Results using the Local Density Approximation (LDA) [16] were conceptually similar showing only minor differences in the calculated total energy values.

Reciprocal space integrations were checked to converge using only Gamma k point for 4 × 4 super-cells with 120 atoms and a vacuum size of 25 Å of vacuum. Van der Waals' interactions were taken into account in the formalism detailed in Refs. [17], as implemented in QE code. The usual dipole correction [18] was applied in all calculations. Relaxation was carried on until forces on each atom had values below 0.002 eV/Angstrom. Graphics were prepared using mainly the XCrysSDen software [19].

2.4.1. Surface model

A large unit cell must be used for the calculations in order to obtain a representative distribution of atom positions that reproduces the electronic properties of an amorphous material. Currently, there are limitations for this kind of calculations due to the large computational resources needed. In spite of this limitation, information can still be obtained at the local spatial scale by analyzing the processes involved in the interaction between molecules and crystal silicon dioxide surfaces. Among the different possible silica polymorphs, β-Cristobalite is the most stable one at high temperatures up to its melting point and it also presents similar properties to those of amorphous silica (e.g. density, refractive index, etc.) [20].

Surface (001) slabs were built starting from an optimized bulk β-Cristobalite crystal structure. The surface chemistry of a silica surface in contact with an aqueous solution is determined to a large extent by the dissociation of the hydroxyl groups. Thus, we simulated a fully hydroxylated surface in all cases, which represents the case of zero surface charge. This usually corresponds to a medium with a pH value between 1 and 2 for the silica surface.

The lattice parameter obtained at the minimum total energy bulk structure was a = 7.463 Å using GGA functional. The distance between silicon atoms and the first neighbor's oxygen atoms was 1.616 Å while the angle formed between O—Si—O atoms was 109.47 degrees. These values obtained are similar to the ones obtained in previous works [20].

We used a 4 × 4 supercell and slab composed by 6 layers of atoms for modeling the crystalline SiO_2 surface. The outermost layer was formed by silicon atoms, each connected to a hydroxyl group, defining in this way a surface with zero net charge. An additional hydrogen back layer was added in order to saturate the oxygen or silicon dangling bonds [21]. Thus the supercell for the clean SiO_2 slab was composed by 120 atoms. The clean slabs were separated by 25 Å of vacuum. All atoms were fully relaxed except the ones belonging to the two deepest layers which were fixed at their bulk ionic positions. Geometries obtained for ions positions after relaxation for the clean slab were similar to previously reported results [20–24].

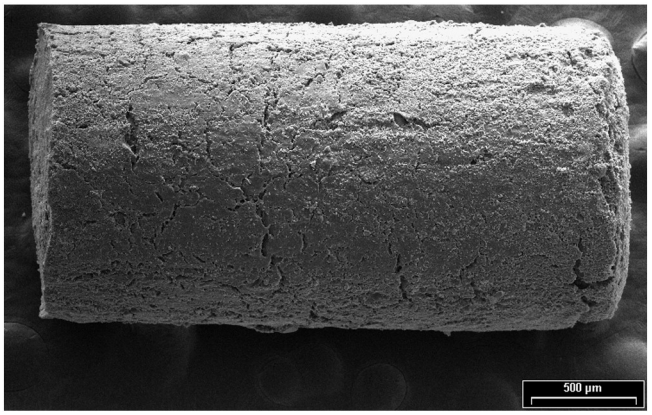

Fig. 1. Cylindrical porous SiO_2 glass pellet.

Table 1
Chemical analysis on the matrix obtained after the leaching test.

Chemical analysis (wt.%)		
Na_2O	Al_2O_3	SiO_2
1.8	3.3	94.8

2.4.2. Adsorption energies

The adsorption energy represents the work that has to be done in order to take the molecule from its original position close to the surface to an infinite distance. For the different systems studied in this work, they were calculated as follows:

$$E_{Ads} = -(E_{Tot} - E_{Sur} - E_{Mol}), \quad (3)$$

where E_{Tot} is the total energy of the fully relaxed system (slab plus the molecule). E_{Sur} is the energy of the optimized clean hydroxylated surface system and E_{Mol} is the energy for an isolated molecule in gas phase at the global minimum. Defined in this way, a positive value for E_{Ads} would imply an adsorbed molecule while a repulsive interaction would be true for a negative value.

Three different cases were analyzed: (1) the silica surface interaction with a CsCl molecule, (2) the silica surface with a sole chlorine atom and (3) the silica surface with a cesium atom. For each case, the relaxed structure was obtained by fully relaxing the slab plus molecule or atom. Different stable positions were found for each case. In order to obtain information about the re-distribution of the electronic charge in the system, the electronic charge transfer D_{Tra} was calculated as

$$D_{Tra} = D_{Sur+Mol} - D_{Sur} - D_{Mol}. \quad (4)$$

Each term of Eq. (4) corresponds to a matrix where each of its elements corresponds to the calculated Löwdin partial charge (Ref. [25]) associated to an atom of that particular configuration. The first term corresponds to the electronic charge distribution found for the relaxed surface plus atom/molecule. The second and the third term correspond to the sole surface and isolated atom respectively, with all its atoms kept at the position reached in the full surface plus atom/molecule configuration.

3. Results and discussion

3.1. Porous glass characterization

The porous SiO_2 glass compacts were characterized chemically and morphologically by scanning electron microscopy (see Fig. 1), and energy dispersive spectroscopy (see Table 1). The cylindrical sintered powder compacts showed a weight loss of 38% during leaching. This value accounts for more than the Na_2O and B_2O_3 content. However some sodium remained in the glass chemical composition, as shown in Table 1. The specific surface area of this glass was determined previously [26] and a value of 40 m^2/g was found.

A SEM micrograph of a cylindrical powder compact is shown in Fig. 1. The obtained structure is the result of sintering and water/acid leaching that removed the phase enriched in B_2O_3 and Na_2O. Fig. 2 shows the sintering porosity observed in the porous SiO_2 glass.

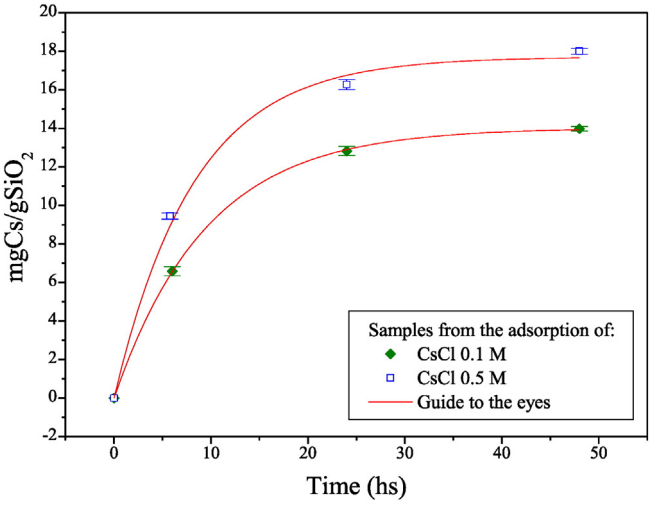

Fig. 3. Mass of adsorbed solute per unit gram of vitreous mass as a function of time. Samples from the adsorption of a) CsCl 0.1 M and b) CsCl 0.5 M (solid lines are a guide to the eyes).

3.2. Adsorption experiments

Adsorbed cesium by unit silica mass was determined from the difference between initial and final ion concentration in the solution where the porous silica samples were placed, as indicated in Section 2.3. Cesium solution concentrations values were measured by atomic absorption spectroscopy. Fig. 3 shows the mass of adsorbed cesium per unit gram of SiO_2 as a function of time.

The porous SiO_2 compacts, placed in the 0.1 M solution, reached an adsorption value of 14 mg of cesium per gram of SiO_2 while the amount of cesium adsorbed on the glass matrix surface placed in more concentrated solution (0.5 M) was 18 mg per gram of glass.

The porous SiO_2 compacts, placed in the 0.1 M solution, reached an adsorption value of 14 mg of cesium per gram of SiO_2 while the amount

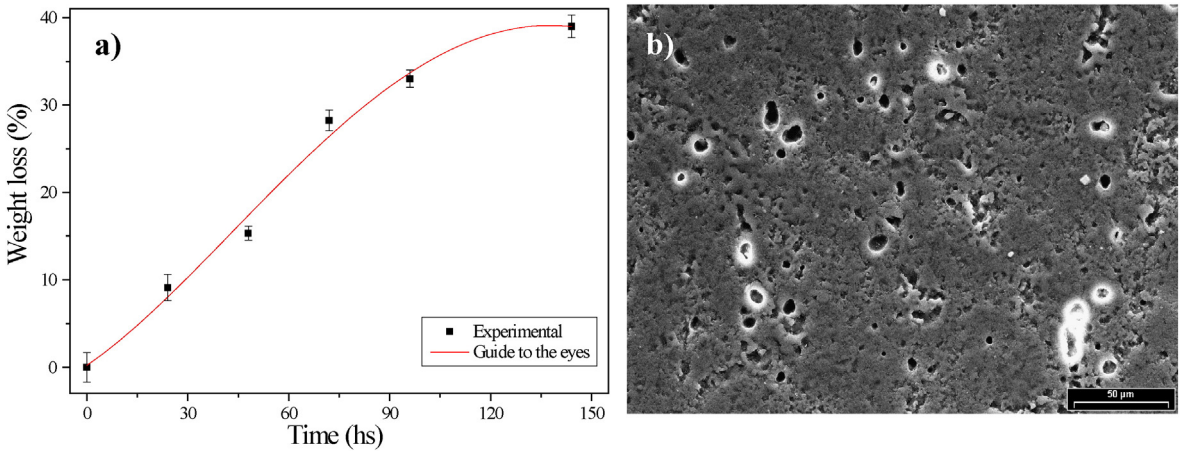

Fig. 2. a) Weight loss during leaching test; b) Scanning electron microscope micrographs of porous SiO_2 glass (solid line is guide to the eyes).

Table 2
Chemical analysis on the matrix obtained after adsorption experiments.

Sample	Chemical analysis (wt.%)				
	Na	Al	Si	Cl	Cs
CsCl 0.1 M	0.61	1.44	89.16	1.28	7.52
CsCl 0.5 M	0.31	1.71	76.14	4.17	17.67

of cesium adsorbed on the glass matrix surface, placed in the concentrated solution (0.5 M), was 18 mg per gram of glass.

For both cases, the maximum adsorbed mass is reached after 48 h of contact of the glass with the solution. Nevertheless, the adsorption kinetics is faster for the more concentrated solution (0.5 M).

Adsorbed cesium at the cylinders surface and at cylinders cross section were determined using energy dispersive spectroscopy (Table 2).

In sample CsCl 0.1 M of Table 2, and at the cylinder surface, the cesium elemental content is 7.5 (in wt.%) and the chlorine elemental content is 1.2 (in wt.%). Meanwhile, on sample CsCl 0.5 M, the cesium elemental content is 17.6 (in wt.%) and the chlorine elemental content is 4.1 (in wt.%) after adsorption experiments. The silicon and cesium distribution, in a transversal cross section of the second sample, was mapped and is shown in Fig. 4. The micrograph obtained by scanning electron microscopy reveals homogeneity in the inner cesium distribution. The adsorption was favored by micrometric porosity from the partial sintering. Nevertheless, the adsorption of CsCl on the outer glass surface and the inner glass surface is not stoichiometric. These results obtained by EDS analysis are supported by the computer simulations based on first-principle calculations, shown in the next Section.

3.3. Density functional theory results

Starting from a fully relaxed slab of hydroxylated Cristobalite SiO_2 surface, adsorption energies were calculated for cesium and chlorine atoms on top of the β-Cristobalite SiO_2 surface.

Two main local minima were found for cesium. The positions at these minima are shown in Fig. 5. For the case shown on the left side, the cesium atoms are located midway along one side of the indicated square shown in the Fig. 5. The length of the side of this square is 5.27 Å. Silicon atoms positioned at the corners, belong to the first surface layer of the crystal. Cesium atoms are positioned symmetrically between two silicon atoms at the vertices at a distance of 3.7 Å. There is

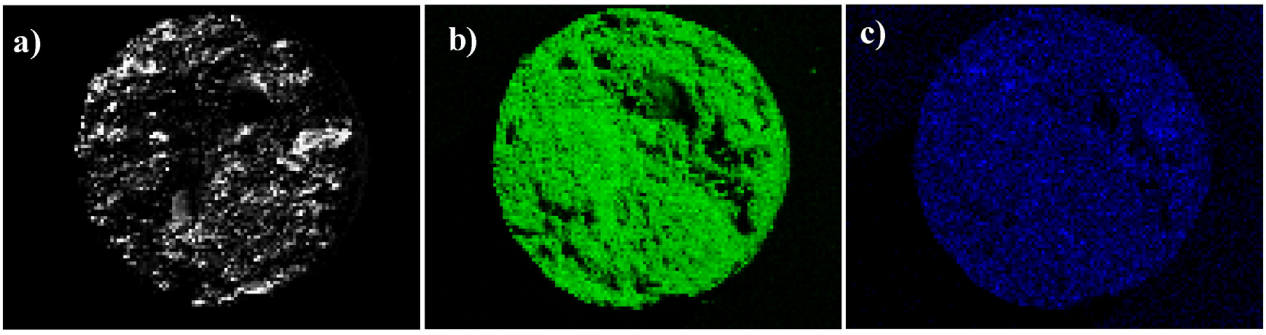

Fig. 4. Cross section of the porous silica glass matrix after 48 h in a CsCl 0.5 M solution. a) Secondary electron scattering on cylinder surface; b) Silicon concentration distribution in an inner cross section and c) Cesium concentration distribution in an inner cross section.

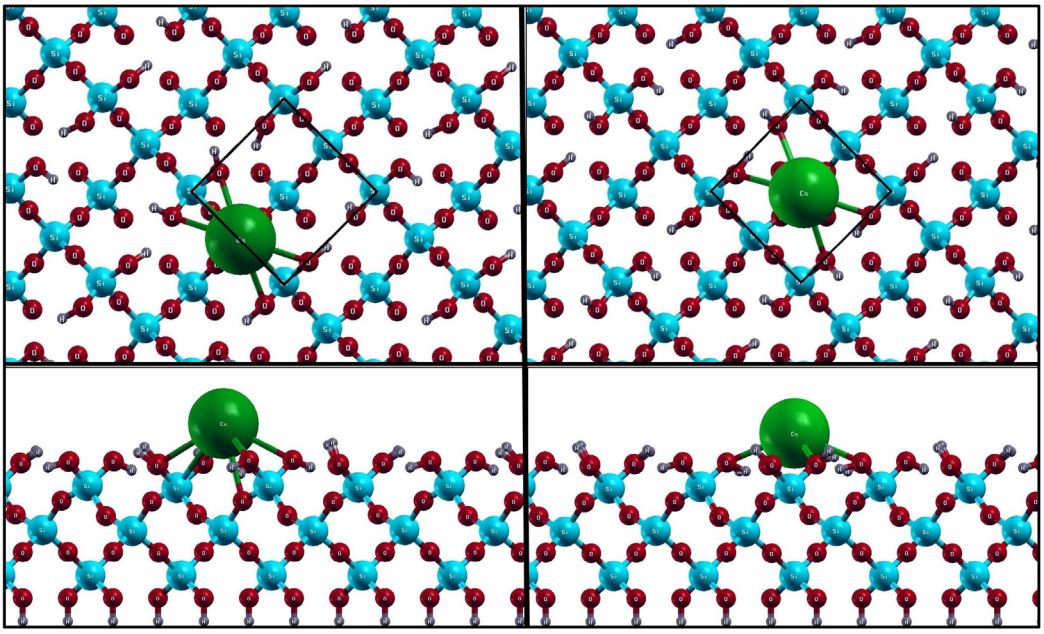

Fig. 5. Relaxed configurations of cesium atom above a SiO_2 β-Cristobalite surface, top view above and the corresponding side view shown below. (Left) The cesium atom is midway on the side of the indicated square with Si atoms at the corner belonging to the first layer of the slab. The calculated adhesion energy is $E_{Ads} = 1.36$ eV. On the right side figures the most stable configuration is shown, with the cesium atom at the center of the square. The calculated adsorption energy is $E_{Ads} = 1.86$ eV.

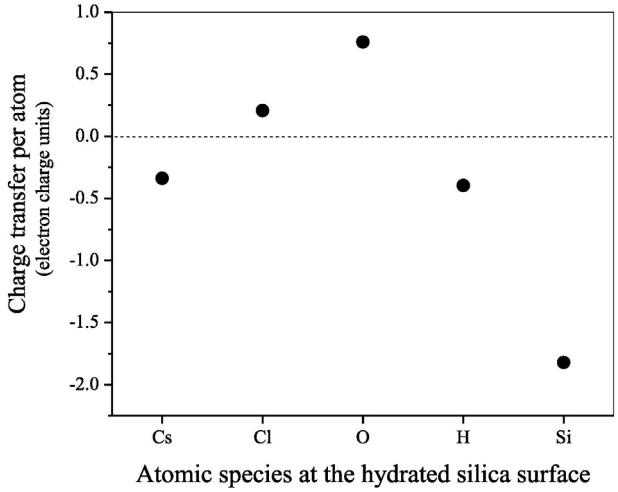

Fig. 6. Eq. (4) allows us to calculate the electronic charge transfer in elemental electron charge units of each atom: of cesium and chlorine adsorbed on the SiO_2 surface, of hydrogen atoms of the hydrated SiO_2 surface, or of silicon and oxygen atoms in the first layers of the Cristobalite slab. Units are in elemental e charge units (e: $1.6 \cdot 10^{-19}$ C). The charges of the isolated atoms were taken as reference and we indicate them by atomic specie. Only 0.3 e migrates out from the cesium atom and 0.2 e flows into the chlorine atom. The effect on the oscillating charge distribution on the surface atoms is minor, thus we indicated the cases for O, Si, and H with the same averaged value for the cases of Cs or Cl on top of SiO_2.

an averaged distance of 3.3 Å from the oxygen atoms belonging to the hydroxiles attached to the former pair of silicon atoms. The adsorption energy for this case is $E_{Ads} = 1.36$ eV.

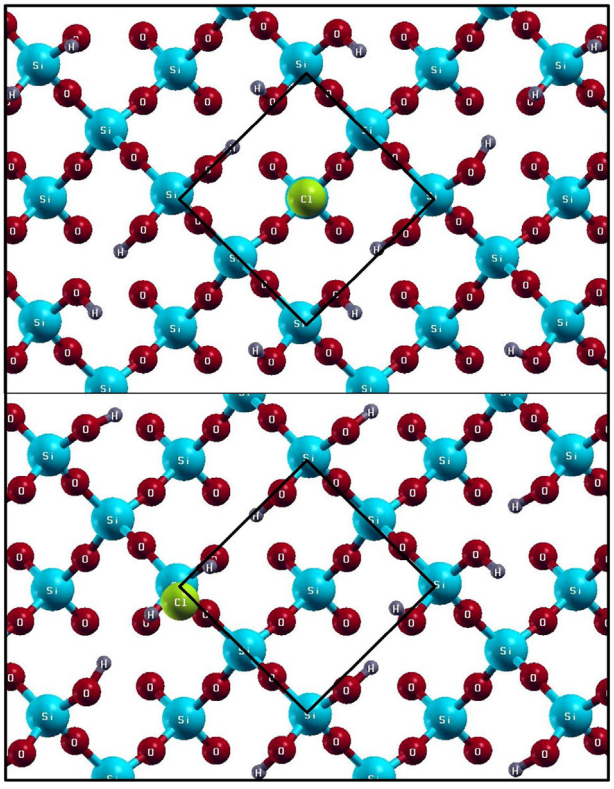

Fig. 7. Energetic favorable positions of chlorine atoms on SiO_2 Cristobalite surface. The marked square has silicon atoms at its vertices that belong to the first surface layer. The atoms on the side are one layer deeper from the surface while the one in the middle belong to the third layer. The calculated adhesion energies are $E_{Ads} = 0.31$ eV for the configuration shown above, where the chlorine atom is at the center of the square. For the configuration below, the chlorine atom is located above the silicon atom at the vertex and an adhesion energy $E_{Ads} = 0.33$ eV was calculated.

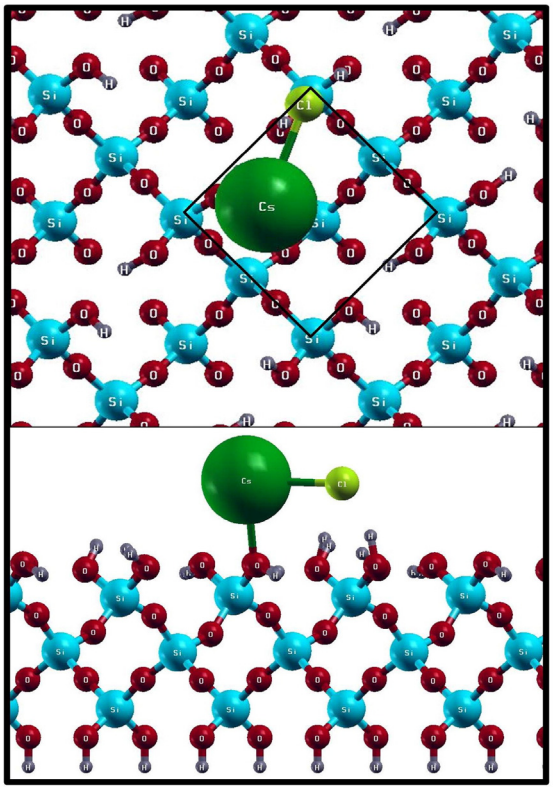

Fig. 8. Most stable configuration found for CsCl molecule. The calculated adhesion energy is $E_{Ads} = 1.89$ eV.

For the other case shown on the right side of Fig. 5, the cesium is located at the center of the suggested square, above a silicon atom that belongs to the third layer of silicon atoms. This case is the most energetically favorable with an adsorption energy per unit cell of $E_{Ads} = 1.86$ eV. Characteristic separation distances in this case are 4.3 Å from the silicon atoms that form the square and 3.3 Å from one of the oxygen atoms belonging to the hydroxyls attached to each of those atoms. The partial Löwdin charges for each atom were obtained and the charge transfer was calculated using the expression shown in Eq. (4). The results indicate a migration of 0.3 e^- out of each cesium. Moreover, the first plane of hydroxiles and silicon dioxide, loose charges as well. These results are shown in Fig. 6 where the charge transfer referenced with respect to the isolated atoms is shown.

Similarly for chlorine, different local minima were found with close values for the total energy of the cell. The positions are shown in Fig. 7. The averaged calculated value for E_{Ads} was 0.33 eV.

For the hypothetical CsCl molecule (see Fig. 8), a global minimum with an E_{Ads} calculated value of 1.89 eV was found.

4. Discussion

The silica glass samples prepared in this work show 38% porosity due to the fact that they were prepared through a simultaneous partial sintering and phase separation process.

Adsorption curves show that the adsorption kinetics is faster for the more concentrated solution. In addition, the adsorption of cesium and chlorine on the surface of the cylinder occurs in a non-stoichiometric way. In particular energy dispersive spectroscopy analysis indicates that the Cs/Cl adsorbed ion ratio is about 6, in the experimental conditions studied.

From the adsorption experiments performed in CsCl 0.1 and 0.5 M solutions at room temperature and at a static regime, we determined that the saturation adsorption of the glass matrices is 14 mg of cesium per gram of glass and 18 mg of cesium per gram of glass, respectively.

Using the results from the first principle calculations, an estimate of the specific adsorption can be obtained. Considering only the most stable attachment sites ($E_{Ads} = 1.86$ eV), their associated area (5.25×5.25 Å) and a specific surface area of 40 m^2/g, the estimate gives a value of 33 mg Cs/g SiO_2. The measured value is half the theoretical estimation. However, the theoretical result comes from a zero temperature calculation from a crystalline phase of SiO_2 while the experiment covers a range of temperatures different from zero with an amorphous SiO_2 sample. Therefore, the estimate reasonably agrees with the measured value.

From the theoretical perspective, we can find the chlorine or cesium attachment sites by computing the energy cost of removing chlorine or cesium atom from the CsCl molecule attached to the SiO_2 surface (see Fig. 8). Using the calculated adsorption energies for cesium (1.86 eV) and chlorine (0.33 eV) plus the expression for the adsorption energy given in Eq. (1), we can deduce that the energy needed for removing a chlorine or cesium atom from the adsorbed CsCl molecule is 4.9 eV and 6 eV, respectively. Thus, it is easier to remove a chlorine atom than a cesium by 1 eV. This result qualitatively supports the experimental results, i.e. the cesium atoms adsorption is favored.

At temperatures greater than 0 K, a quantitative argument can be made if the probability (P) of adsorption of an atom is assumed to follow an Arrhenius type equation, i.e. proportional to $e^{-(-EAds/kT)_B}$. Using the adsorption energies calculated at the most favorable positions for chlorine ($E_{Ads} = 0.33$ eV) and cesium ($E_{Ads} = 1.86$ eV), the ratio (R) between the probabilities for P(Cs) and P(Cl) is given by:

$$R = e^{-(\Delta E/kT)} \tag{5}$$

where:

$$\Delta E = E_{Ads(Cl)} - E_{Ads(Cs)} \tag{6}$$

The calculated value $\Delta E \sim 1.5$ eV implies a ratio (R) favorable to the adsorption of cesium atoms over chlorine ones by many order of magnitude. This result is valid for a wide range of temperatures even at a pH = 1–2 where cesium adsorption is not at its maximum value.

The fully hydroxylated surface, used to calculate the adsorption energies, simulates the system at the isoelectric point of the SiO_2 surface, i.e. pH = 2. However, the experiments were carried at pH = 5, well above the isoelectric point. Consequently, a cesium atom will be affected by a negative charged surface and, based on electronegativity arguments; a stronger adsorption will be expected. It is to be noted that water molecules from the solvent, surrounding the solute ions, were not taken into account.

5. Conclusions

Porous SiO_2 glass matrices were prepared. Water leaching removes most of the B_2O_3 and Na_2O enriched phase. The final result is a SiO_2 porous glass matrix with minor quantities of sodium and aluminum atoms and a specific surface area of 40 m^2/g.

From the adsorption experiments performed in CsCl 0.1 and 0.5 M solutions at room temperature and at a static regime, we determined that the adsorption of the glass matrices is 14 and 18 mg of cesium per gram of glass, respectively. These results are in agreement with theoretical adsorption calculations that take into account the density of attachment sites determined in this work.

The experimental results show that the adsorption of CsCl on the surface of the glass is not stoichiometric. The adsorption of cesium atoms is favored over chlorine atoms.

Theoretical calculations based on Density Functional Theory support, qualitatively, the experimental results. The adsorption energies for cesium atoms are higher than the obtained adsorption energies for chlorine. Therefore, chlorine atoms will be easier to remove from the surface than cesium atoms. More information regarding the cesium adsorption behavior can be obtained from the calculation of the adsorption energy of a hypothetical CsCl molecule on the β-Cristobalite surface. The theoretical results indicate that a chlorine atom is easier to be removed from the adsorbed molecule than the cesium atoms. The result is in agreement with the experimental result giving a Cs/Cl ratio of 6, favorable to the retention of cesium atoms in the glass.

The chemical process that occurs between the molecule and the surface involves important charge redistribution. A charge of 0.3e migrates out from the cesium atom to the SiO_2 slab, and for the case of chlorine a charge of 0.2e flows from the slab to the chlorine atom.

Acknowledgments

This work has been financed by the project PICT 2008-39 and PICT PRH 0102 ANPCyT Argentina. The authors wish to acknowledge all the people who have contributed to the development of this work: Mr. Michele Sanfilippo, Mr. Gustavo Sepúlveda, Mr. Carlos Cotaro, Dr. Jorge Garcés and particularly the Departamento Fisicoquímica y Control de Calidad - Complejo Tecnológico Pilcaniyeu (CNEA) for the equipments provided for the development of this work.

References

[1] M. Aparicio, M.O. Prado, A. Durán, J. Non-Cryst. Solids 352 (2006) 3478–3483.
[2] N. Sadiki, J.P. Coutures, C. Fillet, J.L. Dussossoy, 2006. J. Nucl. Mater. 348 (2006) 70–78.
[3] C.M. Jantzen, J. Non-Cryst. Solids 84 (1986) 215–225.
[4] G. Phillips, R. Russo, Metal Bioaccumulation in Fishes and Aquatic Invertebrates: A Literature Review, United States Environmental Protection Agency, 1978 (PB 290-659).
[5] W. Haller, Chromatography on glass of controlled pore size, Nature 206 (1965) 693–696.
[6] Roy, R. Scientific Basis for Nuclear Waste Management, Vol. 1, Boston 1978, McCarthy (Plenum Press, New York) p.1. (1979).
[7] A. Rimola, M. Sodupe, S. Tosoni, B. Civalleri, P. Ugliengo, Langmuir 22 (2006) 6593.
[8] D. Costa, A. Tougerti, F. Tielens, C. Gervais, L. Stievano, J.F. Lambert, Phys. Chem. Chem. Phys. 10 (42) (2008) 6360.
[9] A. Rimola, M. Sodupe, P. Ugliengo, J. Phys. Chem. C 113 (2009) 5741.
[10] J. Rincón, A. Durán, Separación de Fases en Vidrios, Sociedad Española de Cerámica y Vidrio, 1982.
[11] P. Hohenberg, W. Kohn, Phys. Rev. 136 (1964) B864.
[12] P. Giannozzi, S. Baroni, N. Bonini, M. Calandra, R. Car, C. Cavazzoni, D. Ceresoli, G.L. Chiarotti, M. Cococcioni, I. Dabo, A. Dal Corso, S. de Gironcoli, S. Fabris, G. Fratesi, R. Gebauer, U. Gerstmann, C. Gougoussis, A. Kokalj, M. Lazzeri, L. Martin-Samos, N. Marzari, F. Mauri, R. Mazzarello, S. Paolini, A. Pasquarello, L. Paulatto, C. Sbraccia, S. Scandolo, G. Sclauzero, A.P. Seitsonen, A. Smogunov, P. Umari, R.M. Wentzcovitch, J. Phys. Condens. Matter 39 (2009) 395502.
[13] D. Vanderbilt, Phys. Rev. B 41 (1990) 7892.
[14] J.P. Perdew, K. Burke, M. Ernzerhof, Phys. Rev. Lett. 77 (1996) 3865.
[15] J. Perdew, A. Zunger, Phys. Rev. B 23 (1981) 5048.
[16] D. Ceperley, B. Alder, Phys. Rev. Lett. 45 (1980) 566.
[17] G. Roman-Perez, J.M. Soler, PRL 103 (2009) 096102;
M. Dion, H. Rydberg, E. Schroeder, D.C. Langreth, B.I. Lundqvist, Phys. Rev. Lett. 92 (2004) 246401.
[18] L. Bengtsson, PRB 59 (1999) 12301.
[19] A. Kokalj, J. Mol, Graph. Model. 17 (1999) 176–179.
[20] C. Arasa, P. Gamallo, R. Sayós, Adsorption of atomic oxygen and nitrogen at β-cristobalite (100): a density functional theory study, J. Phys. Chem. B 109 (31) (2005) 14954–14964.
[21] Q. Ma, K. Klier, H. Cheng, J. Mitchell, K. Hayes, Phys. Chem. B 104 (2000) 10618.
[22] T. Akiyama, H. Kageshima, Appl. Surf. Sci. 216 (2003) 270.
[23] I. Baraille, M. Loudet, S. Lacombe, H. Cardy, C.J. Pisani, Mol. Struct. (Theochem.) 620 (291) (2003).
[24] M. Nuñez, M.O. Prado, Adherence of model molecules to silica surfaces: first principle calculations, Phys. Procedia 48 (2013) 214–219.
[25] P.O. Löwdin, Phys. Rev. 97 (1955) 1474–1489.
[26] E. Rivera, Desarrollo de Microesferas cerámicas Porosas Para Aplicaciones en Quimioterapia Interna Selectiva a Tumores MalignosMagister Thesis Instituto Balseiro, 2010.